Journal of Molecular Structure 1346 (2025) 143201

Contents lists available at ScienceDirect

Journal of Molecular Structure

journal homepage: www.elsevier.com/locate/molstr

Eco-friendly polyethylene glycol (PEG-400): PEG mediated synthesis, *in-vitro*, molecular dynamics, DFT, docking, ADMET and MM-GBSA studies of novel sulfonamides as potential antioxidant agents

C.R. Santhosh [a], Sampath Chinnam [a,*], Hrushikesh S. Chaudhari [b], Kondapalli Venkata Gowri Chandra Sekhar [b], Gbolahan O. Oduselu [c], Vishal Ahuja [d], Kumarappan Chidambaram [e], Nagaraju Kerru [f], G.M. Madhu [g,**]

[a] Department of Chemistry, M.S. Ramaiah Institute of Technology (Affiliated to Visvesvaraya Technological University, Belgaum), Bengaluru, Karnataka 560054, India
[b] Department of Chemistry, Birla Institute of Technology and Science, Pilani, Hyderabad Campus, Jawahar Nagar, Kapra Mandal, Hyderabad, Telangana 500078, India
[c] West African Centre for Cell Biology of Infectious Pathogens (WACCBIP), P.O Box LG 54, University of Ghana, Accra, Ghana
[d] Department of Biotechnology, University Centre for Research and Control, Chandigarh University, Mohali, Punjab 140413, India
[e] Department of Pharmacology, College of Pharmacy, King Khalid University, Abha 61421, Saudi Arabia
[f] Department of Chemistry, GITAM School of Sciences, GITAM University, Bengaluru, Karnataka 561203, India
[g] Department of Chemical Engineering, M.S. Ramaiah Institute of Technology (Affiliated to Visvesvaraya Technological University, Belgaum), Bengaluru, Karnataka 560054, India

ARTICLE INFO

Keywords:
Sulfonamides
Antioxidant activity
Molecular dynamics
Docking
DFT
ADMET
MM-GBSA

ABSTRACT

Novel thiomorpholine bearing sulfonamide analogs **3(a-f)** were synthesized by a facile one-pot, single-step process in good to excellent yields (87–95 %). Polyethylene glycol (PEG-400) was used as an eco-friendly, recyclable, and non-flammable solvent. *In-vitro* antioxidant studies were done using H_2O_2 and DPPH radical scavenging assays, while the docking studies were carried out using the Maestro software. In the DPPH assay, the activity of compound **3c** with an IC_{50} value of 30.83±0.33 μg/mL was comparable to the standard, ascorbic acid (13.54±0.33 μg/mL). Interestingly, this compound demonstrated the highest scavenging antioxidant activity at all concentrations, with an IC_{50} value of 32.78±0.33 μg/mL in the H_2O_2 method. Compound **3b,** with salt bridge interactions and hydrogen bonds, exhibited a docking score of -2.01 kcal/mol (PDB: 1H4O). ADME results indicated that all the synthesized compounds obeyed Lipinski's rule, indicating the drug-like properties. The RMSD curve of complex **3b** was observed to be closely matching with benzoic acid, the co-crystallized ligand, indicating alignment and stability with the reference ligand. The optimized molecules with lower energy gaps of 2.17, 4.23, and 1.21 eV indicating that the synthesized compounds shown potent biological activity. This protocol offers excellent yields, green solvent, catalyst-free, shorter reaction times, inexpensive, and no harsh reaction conditions. These research findings reveal that these sulfonamide analogs could be potent antioxidant pharmacophores for future research in antioxidant drug discovery.

1. Introduction

Antioxidants are important health-protecting factors as they fight against reactive free radicals [1]. Free radicals such as hydroxyl, superoxide, and nitric oxide are oxygen-centered radicals, called reactive oxygen species (ROS). They are formed from the side reactions of various biochemical redox reactions inside the body, and they can be noxious when present in excess [2,3]. Free radicals in large quantities can impair lipids, enzymes, DNA, proteins, and tissues. Consequently, this may result in several illnesses, including aging, diabetes, cancer, cardiovascular disease, autoimmune diseases, and neurological disorders [4,5]. Antioxidant molecules interact with free radicals and stop the

* Corresponding author at: Department of Chemistry, M.S. Ramaiah Institute of Technology (Affiliated to Visvesvaraya Technological University, Belgaum), Bengaluru, Karnataka 560054, India.
** Corresponding author at: Department of Chemical Engineering, M.S. Ramaiah Institute of Technology (Affiliated to Visvesvaraya Technological University, Belgaum), Bengaluru, Karnataka 560054, India.
E-mail addresses: sampath@msrit.edu (S. Chinnam), gmmadhu@msrit.edu (G.M. Madhu).

https://doi.org/10.1016/j.molstruc.2025.143201
Received 29 March 2025; Received in revised form 19 June 2025; Accepted 2 July 2025
Available online 3 July 2025

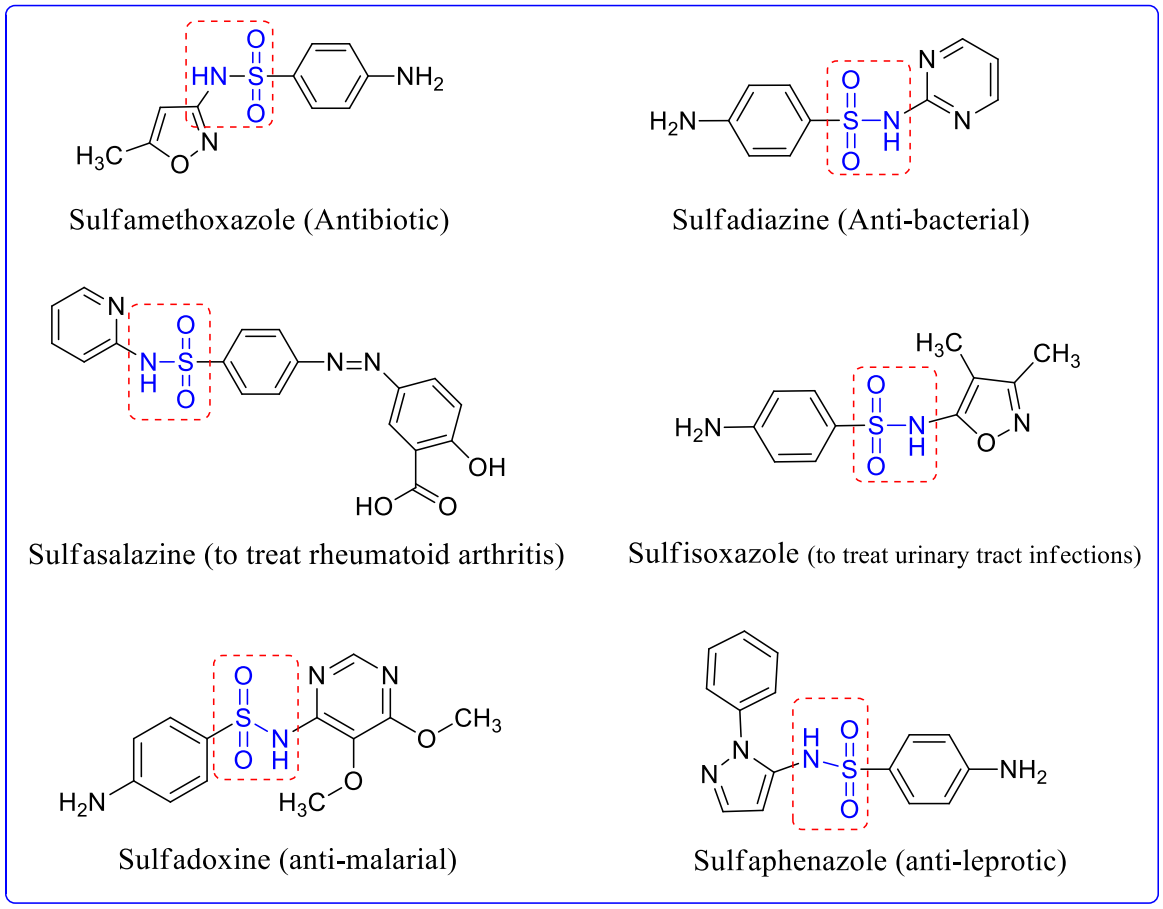

Fig. 1. FDA-approved and marketed sulfonamide-containing drugs.

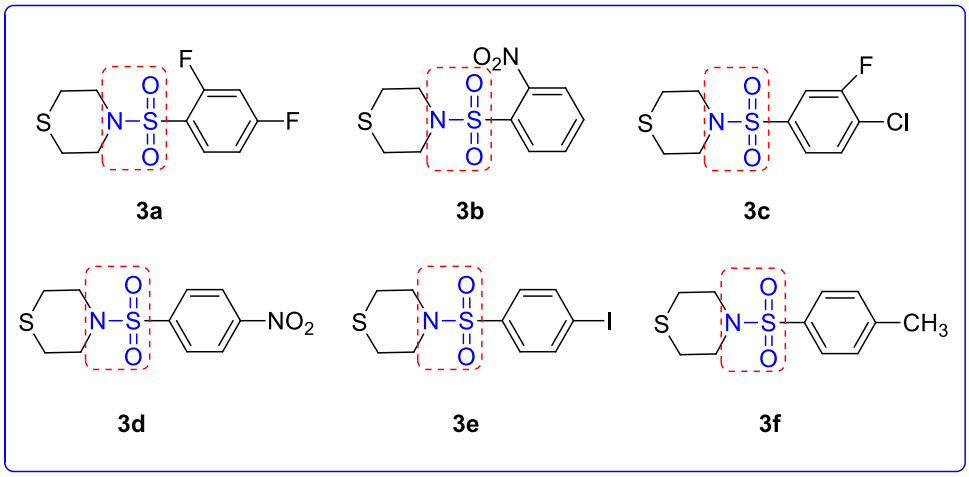

Fig. 2. Our designed sulfonamide analogs containing thiomorpholine **3(a-f)**.

chain reactions, thereby protecting the essential molecules [6]. Consequently, research on developing novel and effective antioxidants with reduced side effects is always a prime focus [7,8].

The morpholine ring contains two different functionalities, such as ether and amine. In thiomorpholine, the oxygen atom is replaced by a sulfur atom [9]. Thiomorpholine scaffold is considered as a leading pharmacophore and has attracted significant attention owing to various applications in biologicals, including anti-fungal [10], anti-viral [11], antioxidant, anti-inflammatory [12], etc. Sulfonamides (sulfa drugs) are amide derivatives, containing the sulfamoyl (-SO_2NH-) group. They are generally synthesized by a one-pot, two-component reaction by sulfonylation of amines with sulfonyl halides using a base [13,14]. They are highly reactive molecules, mostly used as antibiotics and effective chemotherapeutic agents [15,16]. They were reported to have prominent applications as antimicrobial [17], anti-tumor [18], anti-inflammatory [19], HIV protease inhibitors [20], etc. The synergistic action of such biologically active compounds has encouraged researchers to design, synthesize, and study their pharmacological properties [21,22]. In this context, several drugs containing sulfonamides have reached the markets and been effective in their activities

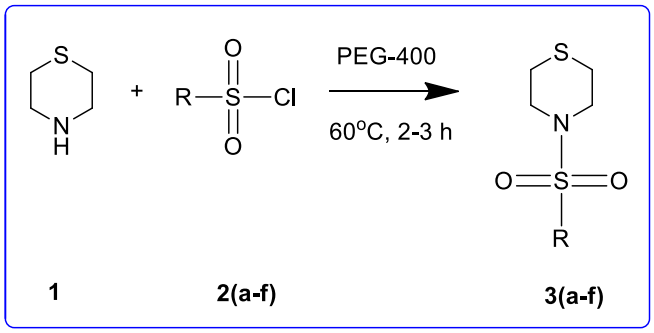

- Eco-friendly solvent
- Shorter reaction times
- No harsh reaction conditions
- No tedious work-up required
- Catalyst-free conditions
- One-pot, two-component methodology
- Excellent yields
- Potent antioxidants
- No column chromatography
- Inexpensive solvent

Compound	R	Time (h)	Yield (%)	Product
3a	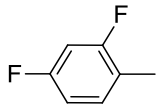	3	89	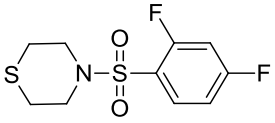
3b	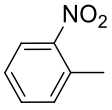	2.0	95	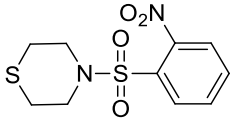
3c	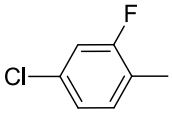	2.5	90	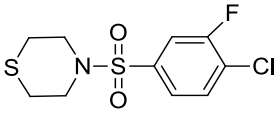
3d	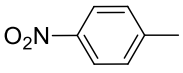	3	91	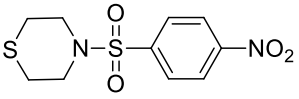
3e	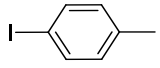	2.5	89	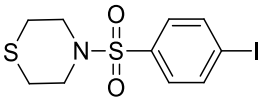
3f	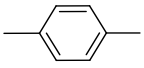	2.0	87	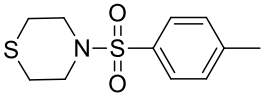

Scheme 1. Synthesis of novel sulfonamide analogs **3(a-f)**.

[23]. Common drugs containing sulfonamides are presented in Fig. 1.

The use of eco-friendly, green solvents for organic synthesis is crucial in a way looking forward to green and sustainable chemistry. Considerable efforts were being made in designing schemes based on solvent-free, water, ionic liquids, polyethylene glycol (PEG) etc., solvent systems [24–26]. PEG has attracted researchers for its non-toxic, non-flammable, inexpensive, and biodegradable properties because it acts as a green solvent. Moreover, it was reported to act as a catalyst for several organic transformations [27,28].

Computational techniques are an important part of drug discovery. As these methods can be employed to virtually screen the designed compounds, to predict their activities on the targeted proteins. Molecular docking gives insights into the interaction types and binding affinities between proteins and ligand molecules [29]. The physicochemical parameters of the molecules, like absorption, lipophilicity, toxicity, etc., can be predicted using ADME studies. Molecular dynamic simulation studies facilitate understanding protein-ligand complex stability, interaction fractions, etc. [30,31]. Likewise, quantum chemical calculations further aid in deducing the molecular properties of the ligands. Therefore, these computational techniques are the

Table 1
Performance of different solvents and temperatures on the synthesis of sulfonamide 3a.

S.No.	Medium	Temp. / °C	Time in hours	% of yields[a]
1	Solvent-free	rt	8.0	9
2	Acetonitrile	rt	8.0	26
3	DMF	rt	6.0	18
4	THF	rt	6.0	31
5	EtOH	rt	6.0	49
6	PEG 400	rt	6.0	61
7	PEG 400	40	4.0	73
8	PEG 400	50	4.0	77
9	PEG 400	60	3.0	89
10	PEG 400	70	3.0	89

Reaction conditions: Thiomorpholine (1.1 mmol), 2,4-difluro-sulfonyl chloride (**2a**, 1.1 mmol), and solvent (5 mL); [a] Isolated yields.

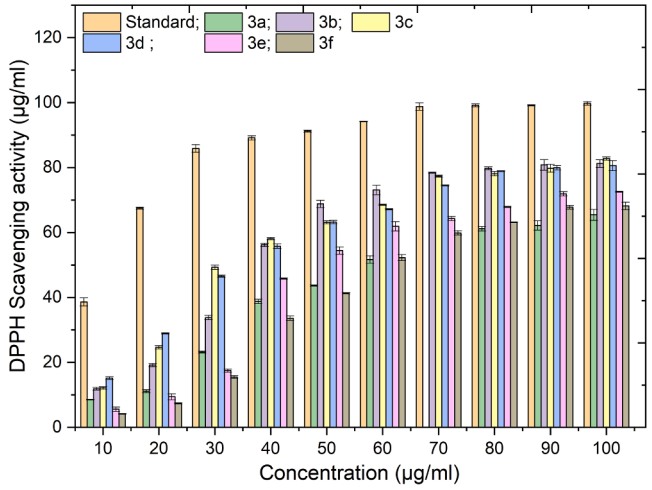

Fig. 3. Scavenging activity of synthesized compounds **3(a-f)** on DPPH radicals at varied concentrations in comparison with the standard drug ascorbic acid.

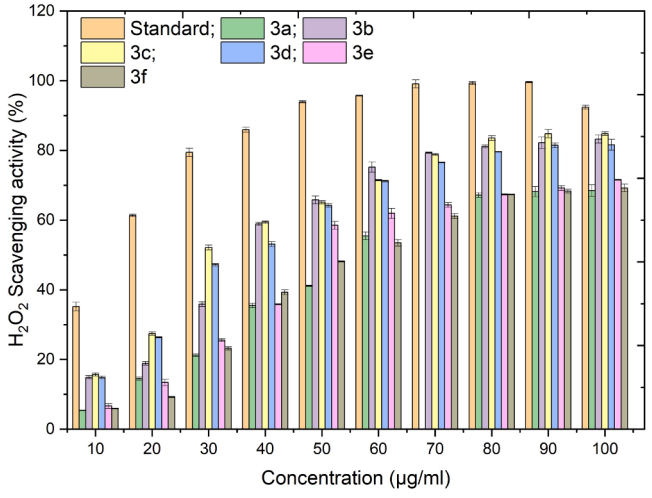

Fig. 4. Percentage scavenging activity of H_2O_2 radicals by the synthesized compounds **3(a-f)** at various concentrations compared with the standard drug ascorbic acid.

key component of medicinal chemistry, supporting effective and safe drugs reaching the market [32,33].

We report a facile, catalyst-free synthesis and pharmacologically potent sulfonamide analogs containing thiomorpholine (Fig. 2) using PEG as a green solvent. *In-vitro* studies were performed by DPPH and H_2O_2 radical scavenging assays to understand their antioxidant properties. Further, *in-silico* ADME, docking, molecular dynamics, DFT, and MM-GBSA calculations were performed on the synthesized compounds to understand their molecular and drug-likeness properties.

2. Materials and methods

2.1

2.1.1. Experimental

The required chemicals thiomorpholine (98 %), and various aromatic sulfonyl chlorides (95–98 %) were purchased from Merck, India, and used without purification. Mel-Temp apparatus with open capillaries was employed to get the melting points of the synthesized compounds, which are expressed in °C (uncorrected). ^{1}H and ^{13}C NMR spectra's were recorded in $CDCl_3$ solvent on a Bruker 400 Avance spectrometer at 400 MHz. Chemical shifts (δ) were expressed in parts per million (ppm) and coupling constants (J) in Hertz (Hz). For HRMS, ambient temperatures and Bruker microTQF-Q II ESI high-resolution was used.

2.1.2. General synthesis procedure of novel sulfonamides 3(a-f)

In a clean 50 mL round-bottom flask, thiomorpholine (0.001 mol) **(1)** was mixed with various aromatic sulfonyl chlorides (0.001 mol) **2(a-f)** in the presence of PEG-400 as a green solvent under catalyst-free conditions at 60 °C for 2–3 h. Reaction completion was monitored by thin-layer chromatography (TLC). Once the reaction was complete, the product was filtered, separated and removed water from PEG by rotary evaporator to get novel sulfonamide analogs containing thiomorpholine **3(a-f)** (Scheme 1) in good to excellent yields (87–95 %).

2.1.3. 4-(2,4-difluorophenylsulfonyl)thiomorpholine (3a)

White solid, Yield: 89 %, mp 156–158 °C. ^{1}H NMR (400 MHz, $CDCl_3$) δ 8.13 (dd, J = 8.1, 1.4 Hz, 1H, Ar-H), 7.75 (td, J = 7.9, 1.4 Hz, 1H, Ar-H), 7.68 (dd, J = 7.8, 1.4 Hz, 1H, Ar-H), 3.07 (t, J = 6.9 Hz, 2H, CH_2), 2.03 (t, J = 7.0 Hz, 2H, CH_2); ^{13}C NMR (100 MHz, $CDCl_3$) δ 135.27, 131.27, 130.64, 130.21, 129.05, 128.82, 128.07, 124.97, 53.21, 27.90; HRMS of $[C_{10}H_{11}NO_2S_2F_2 + H]^+$ (m/z) 280.1294; Calcd: 280.1290.

2.1.4. 4-(2-nitrophenylsulfonyl)thiomorpholine (3b)

Yellow solid, Yield: 95 %, mp 178–180 °C. ^{1}H NMR (400 MHz, $CDCl_3$) δ 8.63 (t, J = 2.1 Hz, 1H, Ar-H), 8.34 (dd, J = 6.2, 0.9 Hz, 1H, Ar-H), 8.21 (dd, J = 2.2, 0.9 Hz, 1H, Ar-H), 7.79 (t, J = 8.2 Hz, 1H, Ar-H), 2.97 (t, J = 8.1 Hz, 2H, CH_2), 1.89 (t, J = 7.9 Hz, 2H, CH_2); ^{13}C NMR (100 MHz, $CDCl_3$) δ 135.20, 131.83, 130.02, 128.07, 125.14, 122.56, 51.89, 26.98; HRMS of $[C_{10}H_{12}N_2O_4S_2 + H]^+$ (m/z) 289.1337; Calcd: 289.1341.

2.1.5. 4-(4-chloro-2-fluorophenylsulfonyl)thiomorpholine (3c)

White solid, Yield: 90 %, mp 178–180 °C. ^{1}H NMR (400 MHz, $CDCl_3$) δ 7.82 (d, J = 2.1 Hz, 1H, Ar-H), 7.59 (dd, J = 8.3, 2.1 Hz, 1H, Ar-H), 7.42 (d, J = 8.3 Hz, 1H, Ar-H), 2.97 (t, J = 8.0 Hz, 2H, CH_2), 1.89 (t, J = 8.0 Hz, 2H, CH_2); ^{13}C NMR (100 MHz, $CDCl_3$) δ 132.50, 130.58, 130.12, 130.02, 127.99, 124.90, 121.28, 121.10, 52.76, 28.18; HRMS of $[C_{10}H_{11}NO_2S_2FCl + H]^+$ (m/z) 295.1445; Calcd: 295.1447.

2.1.6. 4-(4-nitrophenylsulfonyl)thiomorpholine (3d)

Yellow solid, Yield: 91 %, mp 187–189 °C. ^{1}H NMR (400 MHz, $CDCl_3$) δ 8.90 (d, J = 7.5 Hz, 2H, Ar-H), 8.20 (d, J = 8.0 Hz, 2H, Ar-H), 2.92 (t, J = 8.0 Hz, 2H, CH_2), 2.07 (t, J = 8.0 Hz, 2H, CH_2); ^{13}C NMR (100 MHz, $CDCl_3$) δ 130.51, 128.91, 128.00, 126.28, 51.92, 26.18; HRMS of $[C_{10}H_{12}N_2O_4S_2 + H]^+$($m/z$) 289.9911; Calcd: 289.9906.

2.1.7. 4-(4-iodophenylsulfonyl)thiomorpholine (3e)

White solid, Yield: 89 %, mp 190–192 °C. ^{1}H NMR (400 MHz, $CDCl_3$) δ 8.36 (d, J = 8.5 Hz, 2H, Ar-H), 7.86 (d, J = 8.5 Hz, 2H, Ar-H), 2.93 (t, J

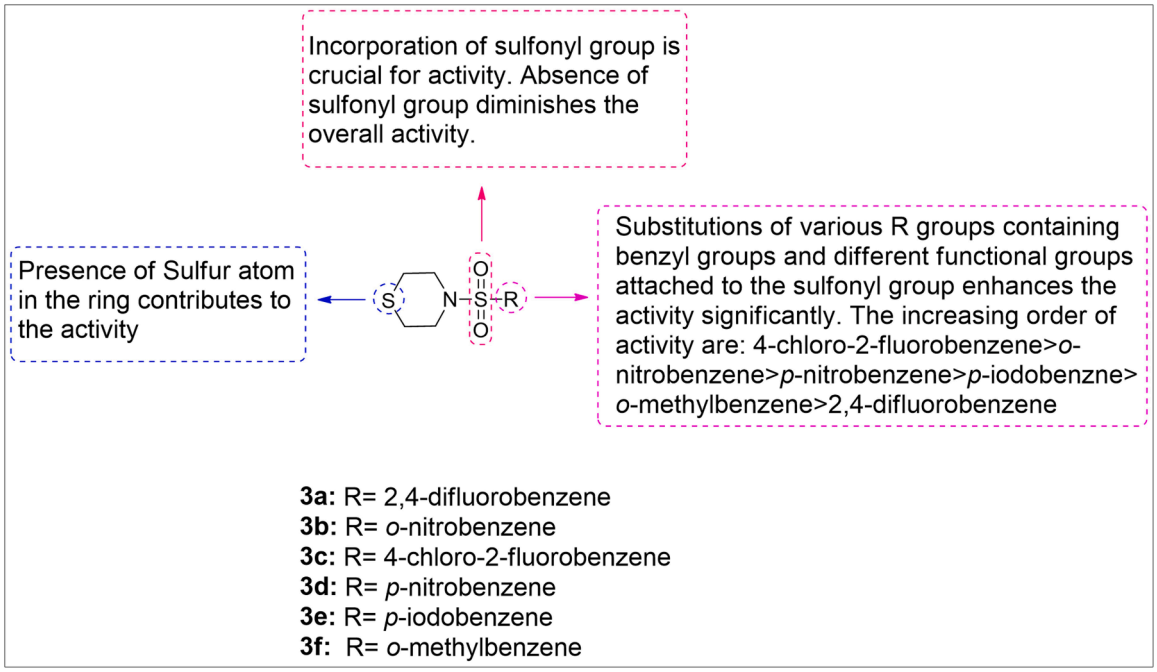

Fig. 5. Structure-activity relationship (SAR) studies of novel sulfonamide analogs **3(a-f).**

Table 2
Predicted ADMET properties of the synthesized compounds 3(a-f).

S. No.	Compound	MW	Log P	HBD	HBA	TPSA	RB	nAH	MR
1	3a	279.33	1.69	0	5	71.06	2	6	66.16
2	3b	288.34	1.35	0	5	116.88	3	6	75.07
3	3c	295.78	2.22	0	4	71.06	2	6	71.21
4	3d	288.34	1.32	0	5	116.88	3	6	75.07
5	3e	369.24	2.14	0	3	71.06	2	6	78.96
6	3f	257.37	1.86	0	3	71.06	2	6	71.21

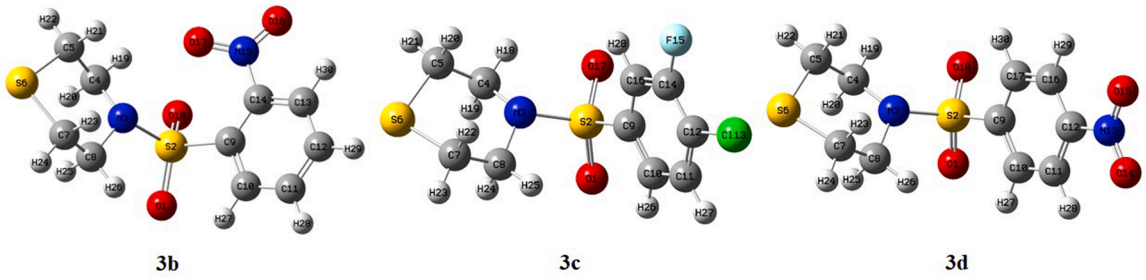

Fig. 6. Geometry optimized compounds **3b, 3c**, and **3d** (B3LYP/6–311G* level).

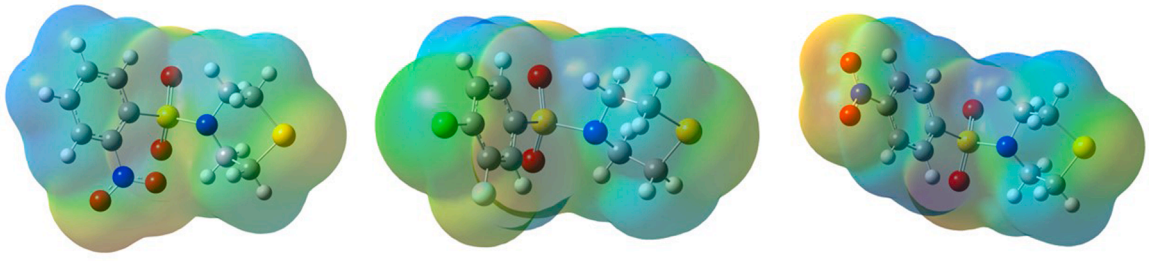

Fig. 7. Molecular electrostatic potential analysis of compounds **3b, 3c,** and **3d** by color range (in a.u.) (Iso-surface ±0.002 a.u).

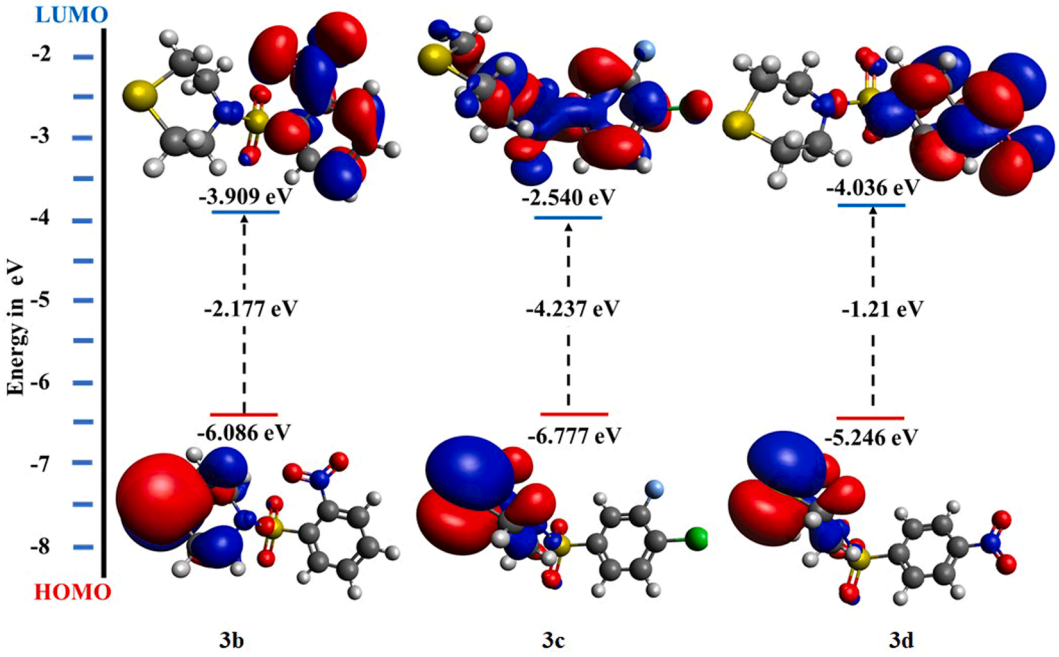

Fig. 8. HOMO-LUMO band gap calculations **3b, 3c,** and **3d** of optimized ligands.

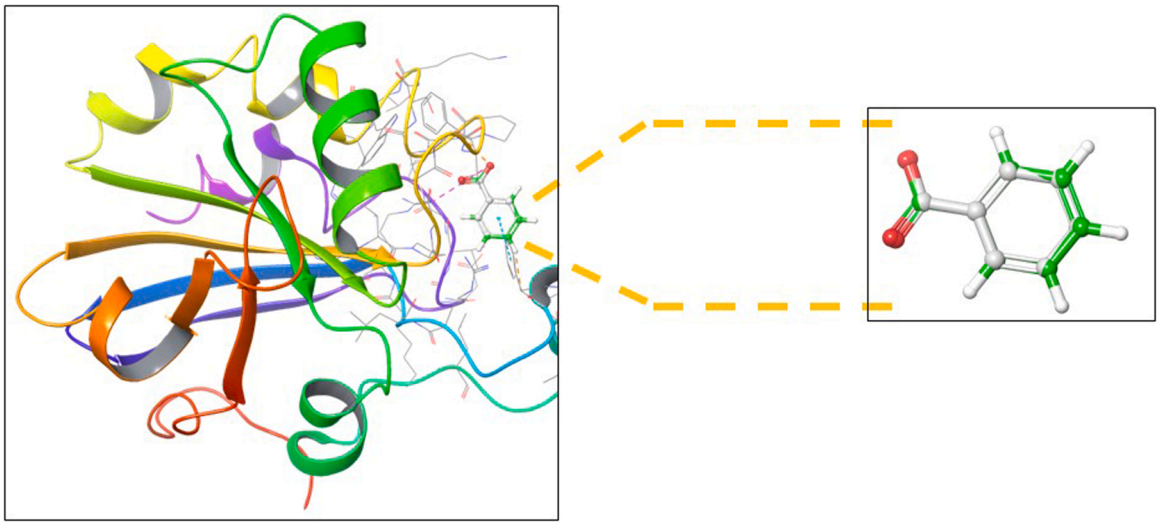

Fig. 9. Validation of docking protocol by re-docking benzoic acid (co-crystallized ligand).

= 7.8 Hz, 2H, CH_2), 2.07 (t, J = 7.9 Hz, 2H, CH_2); ^{13}C NMR (100 MHz, $CDCl_3$) δ 129.51, 123.36, 122.09, 121.30, 52.91, 29.95; HRMS of $[C_{10}H_{12}NO_2S_2I + H]^+$ (m/z) 369.1486; Calcd: 369.1487.

2.1.8. *4-tosylsulfonylthiomorpholine (3f)*

White solid, Yield: 87 %, mp 190–192 °C. ^{1}H NMR (400 MHz, $CDCl_3$) δ 7.38 (d, J = 8.3 Hz, 2H, Ar-H), 6.89 (d, J = 8.3 Hz, 2H, Ar-H), 2.89 (t, J = 8.1 Hz, 2H, CH_2), 2.31 (s, 3H, CH_3), 2.08 (t, J = 8.0 Hz, 2H, CH_2); ^{13}C NMR (100 MHz, $CDCl_3$) δ 124.67, 123.09, 121.89, 120.51, 52.79, 28.38, 18.15; HRMS of $[C_{10}H_{15}NO_2S_2 + H]^+$ (m/z) 258.0689; Calcd: 258.0698.

2.2. *Biological studies*

2.2.1. *In-vitro antioxidant studies*

The antioxidant activity of compounds **3(a-f)** was assessed using the DPPH free radical scavenging assay [34]. To compare the antioxidant activity of these compounds, ascorbic acid was treated as a positive control. A 0.004 % DPPH solution was obtained by mixing 4 mg of it in 100 mL of methanol. A series of solutions with different concentrations (10, 20, 30, 40, 50, 60, 70, 80, 90, and 100 µg/mL) of the synthesized compounds were obtained by diluting them with methanol. Each of the test solutions (1 mL) was mixed with 4 mL of DPPH: methanol solution. Samples were incubated for 30 min in the dark. Using a UV–visible spectrophotometer, the sample's absorbance was measured at 517 nm. The scavenging activities of the samples were computed by the following equation.

$$\%\ Inhibition\ of\ DPPH = \frac{(Abs_{control} - Abs_{sample})}{Abs_{control}} \times 100$$

Where '$Abs_{control}$' indicates the DPPH solution absorbance and 'Abs_{sample}' defines the sample and the DPPH solution's absorbance.

Synthesized compounds **3(a-f)** were also examined for the hydrogen peroxide radical scavenging activity [35]. A hydrogen peroxide solution of 40 mM was obtained in phosphate buffer (pH=7.4–7.5). Test

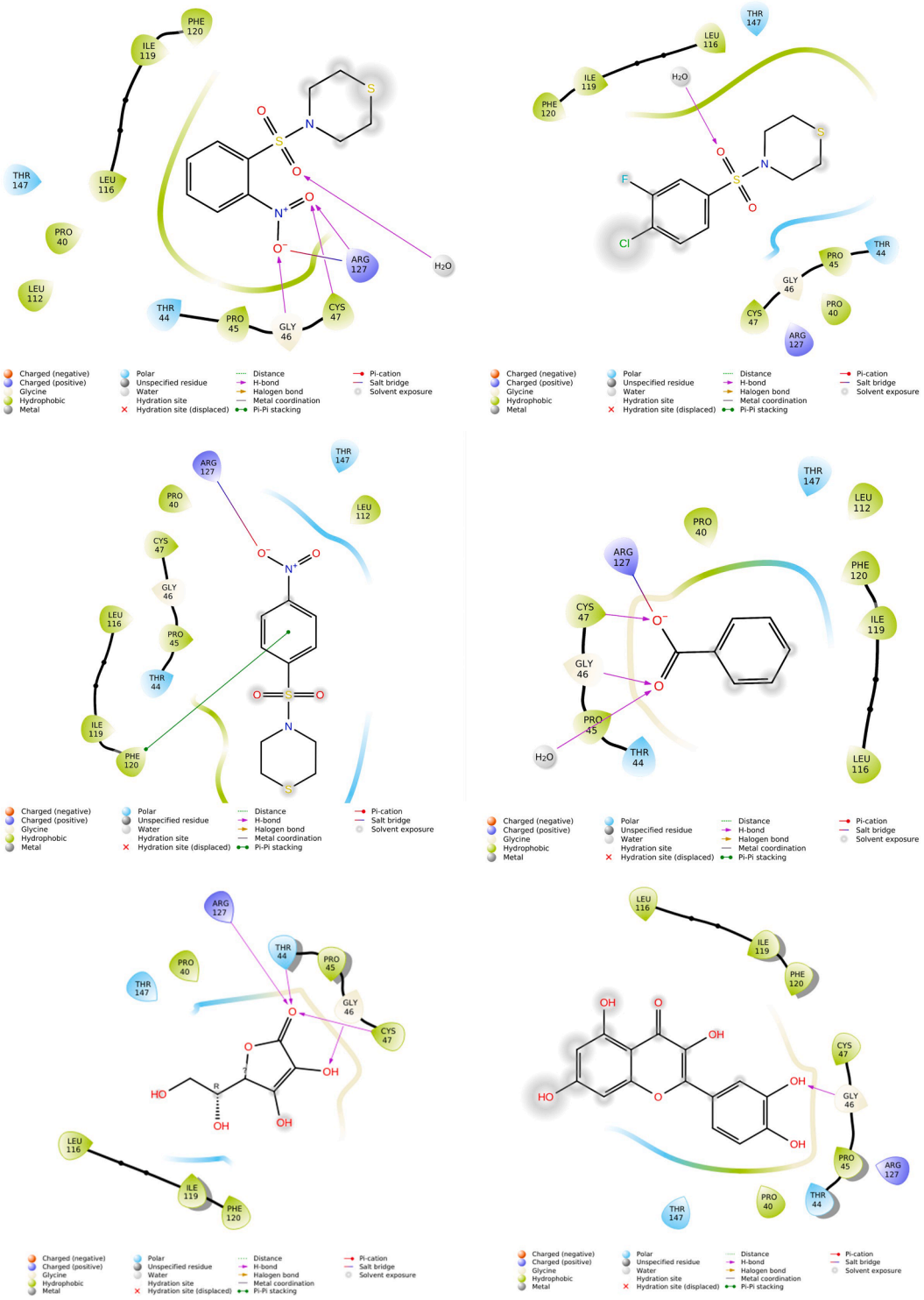

Fig. 10. Docking poses of **3b, 3c, 3d, BA, ascorbic acid, and quercetin** with targeted protein.

compounds in 3.4 mL of phosphate buffer were added to the H_2O_2 solution (0.6 mL, 40 mM). Dark incubation (30 min) was carried out for the samples. Samples and phosphate buffer's absorbance values were then measured without hydrogen peroxide at 230 nm by a UV spectrophotometer. As a standard, ascorbic acid was employed. The scavenging activity of the hydrogen peroxide radical was computed using the given formula.

$$\%\ Inhibition\ of\ H_2O_2 = \frac{(Abs_{control} - Abs_{sample})}{Abs_{control}} \times 100$$

Where $Abs_{control}$ indicates standard H_2O_2 absorbance; Abs_{sample} describes the absorbance values in the presence of the sample and standard H_2O_2.

In both methods, IC_{50} values were obtained from a plot between the concentration of test compounds and the percentage of scavenging activity.

Table 3
Docking scores, interaction types with amino acids of the co-crystal ligand (BA) and potent compounds.

Compound	Amino acid involved	Type of bond	Distance (Å)	Dock score (kcal/mol)
BA (Co-crystallized)	GLY 46	H-Bond	1.98	−5.27
	CYS 47	H-Bond	2.29	
	ARG 127	Salt bridge	3.42	
3b	GLY 46	H-Bond	2.16	−2.01
	CYS 47	H-Bond	1.83	
	ARG 127	H-Bond	1.86	
	ARG 127	Salt bridge	3.34	
3c	–	–	–	−1.99
3d	PHE120	Pi-Pi stacking	5.35	−2.07
	ARG 127	Salt bridge	2.09	
Ascorbic acid	GLY 46	H-Bond	2.10	−6.67
	CYS 47	H-Bond	1.93	
	THR 44	H-Bond	1.76	
	ARG 127	Salt bridge	3.04	
Quercetin	GLY 46	H-Bond	2.31	−5.58

2.3. In-silico ADMET

SwissADME and pkCSM tools were used to predict the ADME properties of the synthesized compounds **3(a-f)**. ChemDraw Ultra 22.0.0 software was employed to draw the 2D structures of the compounds. And they were converted into SMILES notations, and further used for analysis [36,37].

2.4. MM-GBSA calculations

Gaussian 09 and GaussView 6.0 were used to analyze the compounds' molecular structures. The molecular properties of the ligands were evaluated by Quantum chemical calculations. Optimization of the ground-state geometric parameters was achieved by the DFT method at the B3LYP/6–311G* level. GaussView 6.0 was employed to visualize the MEP and FMOs [38,39].

2.5. Molecular docking studies

Docking investigations were performed on the three molecules that demonstrated the highest antioxidant activity. Using Maestro 2022–1 version 4.2.667, Glide XP docking was employed to evaluate the compatibility and interactions of thiomorpholine-based sulfonamides with the PrxV receptor (PDB: 1H4O). Molecules were docked using Glide XP at the PrxV receptor's active sites [40–43].

2.6. Molecular dynamics (MD) studies

Desmond v5.9 (Schrödinger 2019–3) was used to perform MD simulations to understand the effects of solvent on the interactions of the protein-ligand complex. Simulation data were recorded every 10 ps, and the NPT ensemble was run for 100 ns. Interaction diagrams were analyzed to study trajectories and frame variations [44–46].

3. Results and discussion

3.1. Chemistry

A novel series of thiomorpholine-containing sulfonamide analogs **3 (a-f)** were synthesized in good to excellent yields (87–95 %) by the reaction of thiomorpholine **(1)** with various aromatic sulfonyl chlorides **2 (a-f)** using PEG-400 as a green solvent under catalyst-free conditions. Reaction conditions were optimized for variables like different mediums, time, and temperature to get maximum yields.

Initially, a pilot reaction was conducted with an equimolar mixture of thiomorpholine (**1**) and 2,4-difluorosulfonyl chloride (**2a**) in 5 mL of solvent (Table 1). Subsequently, a detailed examination focused on the influence of varying solvents and the impact of temperature was done. Initially, the reaction was carried out at room temperature in reflux condition for 8 h without any medium, and no product was observed (Table 1, entry 1); it indicates the essential role of a medium for the successful transformation to the desired product. The reaction was then explored using different aprotic solvents (Acetonitrile, DMF, and THF). When comparing the aprotic medium, a low-yielding product was obtained even after extended reaction times for 8 h (Table 1, entries 2–4). Further, a moderate yield of product was observed by using protic solvent, ethanol (Table 1, entry 5). Surprisingly, PEG-400 yielded markedly superior results (61 %), establishing PEG-400 as the most effective medium and as an activator for the one-pot benchmark reaction (Table 1, entry 6).

Further investigations into the optimal temperature conditions for the model reaction were conducted. The reaction rate accelerated noticeably with a temperature increase from room temperature to 70 °C, which also significantly enhanced the yield of the expected product. It was particularly encouraging to note that at a moderate temperature range of 60 °C, the reaction proceeded smoothly and yielded almost complete conversion of the reactants. This temperature range facilitated the production of the desired product (**3a**) with an impressive 89 % yield for 3 h (Table 1, entries 7–10). Subsequent temperature elevation showed no further improvement in the product yield, affirming that 60 °C is the most efficient temperature for this transformation.

Spectral techniques such as ^{1}H, ^{13}C NMR and HR-MS confirmed the formation of the designed compounds. In ^{1}H NMR, peaks at δ 7.38–8.90 ppm were assigned for the aromatic hydrogen atom of compounds **3(a-f)**. Doublets were shown at δ 6.89–8.34 ppm corresponding to aromatic protons for **3(a-f)** compounds. Further, doublets appeared at δ 7.42–8.21 ppm, confirming protons in the aromatic ring of **3(a-c)** compounds. Triplets were seen at δ 2.89–3.07 ppm, which was attributed to the $–CH_2$ group of **3(a-f)** compounds. Peaks at δ 1.89–2.08 ppm were assigned for the $–CH_2$ group of **3(a-f)** compounds. In the ^{13}C NMR spectrum, all the signals corresponding to aromatic carbon were observed in the expected δ range from 120.0–135.0 ppm. Also, carbon peaks of the $-CH_2-$ group were observed in the ranges of δ 25.0–55.0 ppm. Additionally, the *m/z* peaks in the HRMS spectra confirmed the formation of all the compounds.

3.2. Biological assay

3.2.1. In-vitro analysis

Scavenging activities of the synthesized compounds **3(a-f)**, on DPPH and H_2O_2 free radicals were evaluated at serial concentrations of 10, 20, 30, 40, 50, 60, 70, 80, 90, and 100 μg/mL. Activity results were compared with the ascorbic acid standard. Scavenging results indicated that the majority of the compounds exhibit good to promising antioxidant activities. The order of DPPH free radical scavenging activity of these compounds was found to be **3c>3b>3d>3e>3f>3a** based on inhibition percentage values. Results disclosed that compounds **3b, 3c,** and **3d** had higher scavenging activity at all concentrations in comparison to other compounds. In particular, compound **3c** had a maximum inhibition percentage of 82.8 ± 0.43 % at 100 μg/mL, these results were comparable with those of the standard at that concentration. We also calculated corresponding IC_{50} values for these compounds and found them to be 35.61±0.45, 30.83±0.33, and 33.52±0.19 μg/mL for **3b, 3c,** and **3d** compounds, respectively. Generally, higher scavenging activity trends are associated with lower IC_{50} values, indicating greater potency to inhibit free radicals. From this study, it was observed that these compounds exhibit lower IC_{50} values. This implies that for 50 % inhibition of respective free radicals, smaller concentrations of compounds were required, indicating their potency. **Table S1** and Fig. 3 outline the percentage of scavenging activity of the synthesized compounds **3(a-f)** at various concentrations.

In H_2O_2 radical scavenging studies, we found the order of percentage

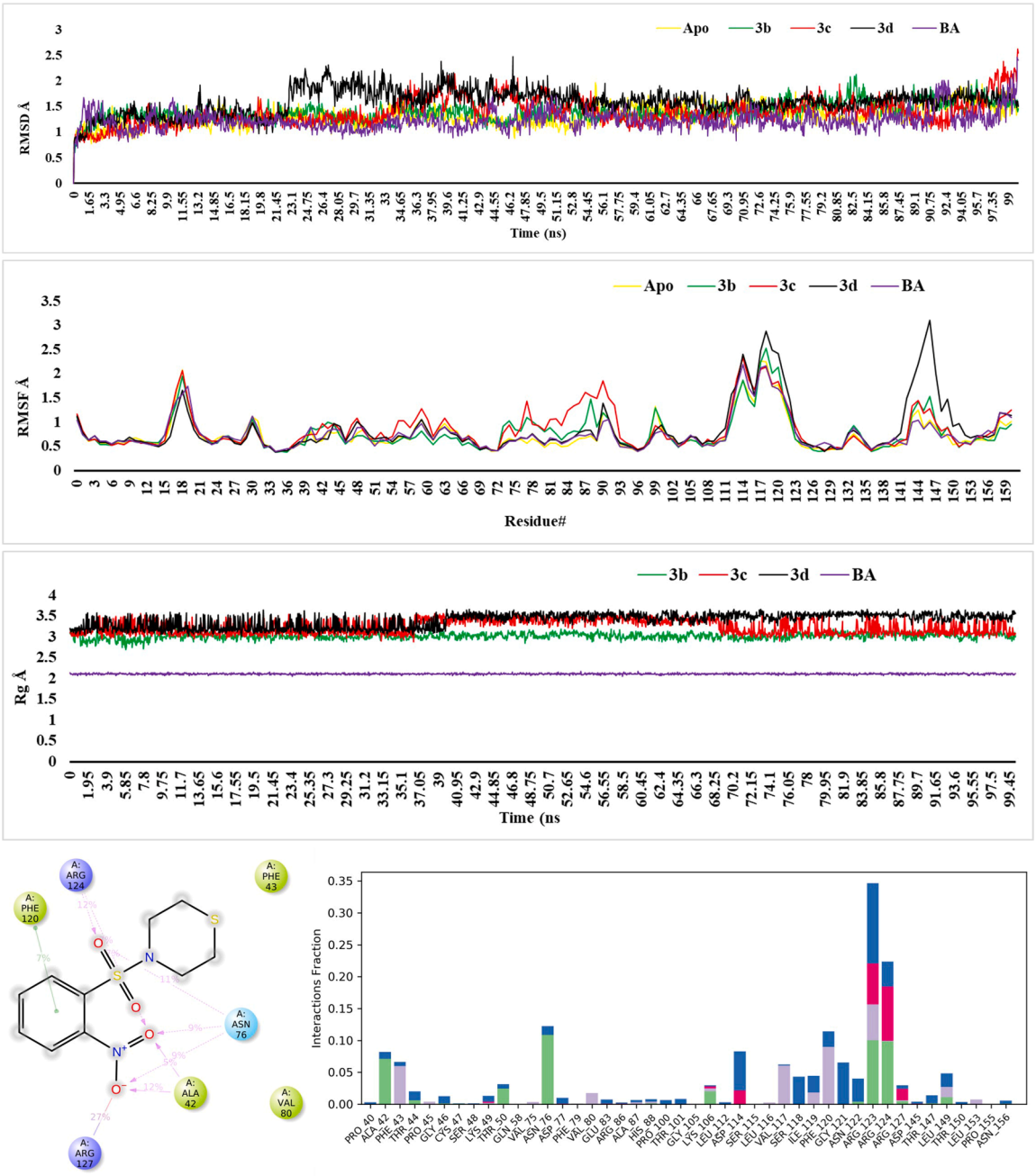

Fig. 11. (**A**) RMSD plot of simulated compounds. (**B**) RMSF plot of 3b, 3c, and 3d, along with BA. (**C**) Rg plot of MD-simulated compounds. (**D**) Protein-ligand interaction fractions of the **3b** complex throughout MDS.

inhibition among the synthesized compounds to be **3c>3b>3d>3e>3f>3a**. Specifically, compound **3c** presented the highest inhibition percentage at almost all the concentrations in comparison to other compounds. The percentage inhibition of compound **3c** at 100 µg/mL was 84.8 ± 0.73 %, comparable with the standard at that concentration (92.42±0.43 %). However, compounds **3b** and **3d** also exhibited significant activity, as the percentage of inhibition was comparable with that of the standard. As discussed earlier, these compounds demonstrated lower IC_{50} values (**3c**: 32.78±0.33 µg/mL, **3b**: 36.05 ±0.61 µg/mL, and **3d**: 34.78±0.43 µg/mL) indicating their potency in inhibition of free radicals. **Table S2** and Fig. 4 outline the H_2O_2 radical scavenging activities of compounds **3(a-f)** at varied concentrations.

Structure-activity relationship (SAR) studies

The structure-activity relationship (SAR) studies of the synthesized novel sulfonamide analogs **3(a-f)** are presented in Fig. 5. From Fig. 5, it is evident that the presence of the sulfonyl group is very crucial for the activity. The sulfur atom present in the ring contributes to activity, and overall thiomorpholine scaffold shows good activity. Activity has enhanced significantly when various substitutions of R groups containing benzyl groups and different substitutions of functional groups at various positions on the benzyl group are clubbed to the sulfonyl group. The order of increasing activity of all the synthesized novel sulfonamide analogs with R groups follows as: **3c**:4-chloro-2-fluorobenzene>**3b**:*o*-nitrobenzene>**3d**:*p*-nitrobenzene>**3e**:*p*-nitrobenzene>**3f**:*o*-methylbenzene>**3a**:2,4-difluorobenzene.

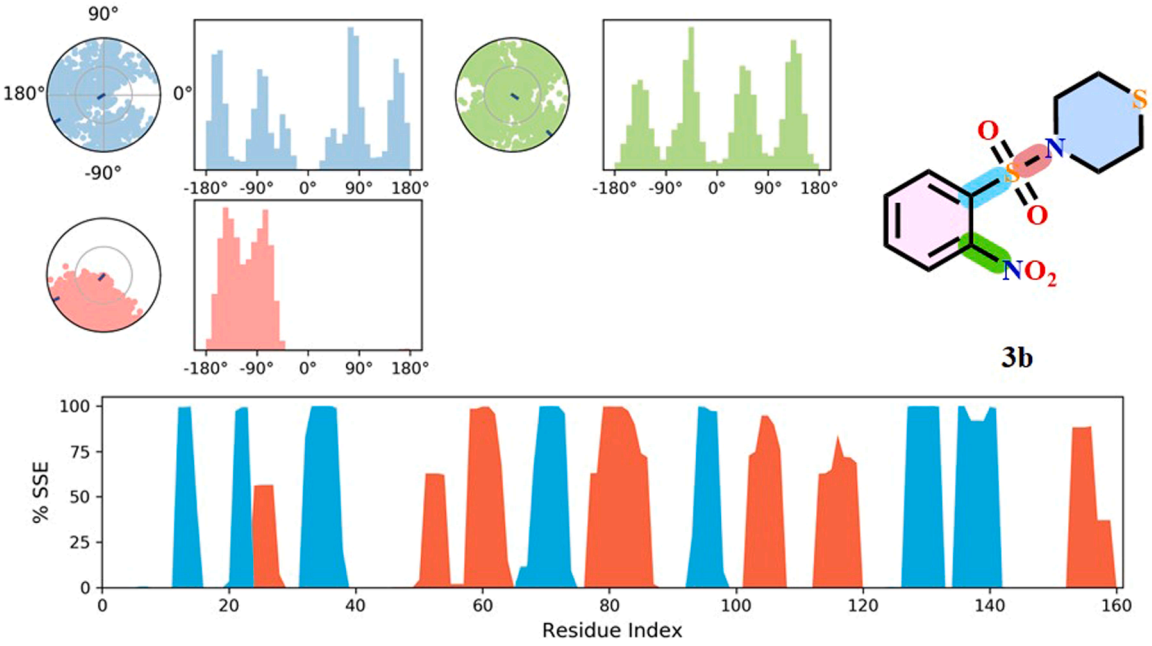

Fig. 12. The secondary structural and torsional profile of the **PrxV-3b** complex.

Table 4
Ligand properties of the simulated ligands.

Compound	RMSD Å	Rg Å	Intra HB	Mol SA sq. Å	SASA sq. Å	PSA sq. Å
3b	1.3976	3.0220	0	233.931	249.309	123.446
3c	1.1806	3.2431	0	232.017	306.930	68.600
3d	0.8499	3.3970	0	237.931	287.405	161.613

Table 5
Pre- and post-simulation binding free energies of BA (co-crystal ligand), **3b, 3c,** and **3d.**

S. No.	Compound	Pre-MDS-binding free energy (kcal/mol)	Post MDS-binding free energy (kcal/mol)
1	**BA**	−22.94	−6.32
2	**3b**	−29.12	−15.61
3	**3c**	−30.33	−30.56
4	**3d**	−39.19	−16.26

3.3. *In silico predicted ADMET properties*

All the synthesized compounds **3(a-f),** were evaluated for their drug-likeness and ADMET properties. This includes count of aromatic heavy atoms (nAH), molecular weight (M.W.), hydrogen bond acceptors (HBA), number of rotatable bonds (R.B.), topological polar surface area (TPSA), molecular refractivity (M.R.), LogP, hydrogen bond donors (HBD), and octanol/water partition coefficient (iLOGP). ADME analysis validated that all the compounds follow Lipinski's Rule of Five with zero violations. This demonstrates the suitability for further studies and drug-like properties of these compounds, as shown in Table 2. The predicted *in-silico* ADME properties disclosed the important physicochemical characteristics of these compounds and are presented in supplementary data (Tables S3 and S4).

3.4. *Geometry optimization of ligands*

Quantum chemistry techniques were used to analyze the molecular geometries of the compounds. Tuning of ligands was done to produce lower-energy and stable molecular structures, which is common in computational research, as shown in Fig. 6. In detail, the labelled optimized structure of compound **3b** is shown in the supplementary file **(Figure S19)**.

3.5. *Molecular electrostatic potential (MEPs) diagrams*

The ground state distributions of charge across the complete energy surface of molecules are explained by MEPs. They are essential for interpreting a molecule's electronic structure. A study on structure-property relationships by indicating the polarity of molecules from coloration is done by MEP analysis. Red, yellow, blue, and green, respectively, stand for negative, slightly negative, positive, and neutral

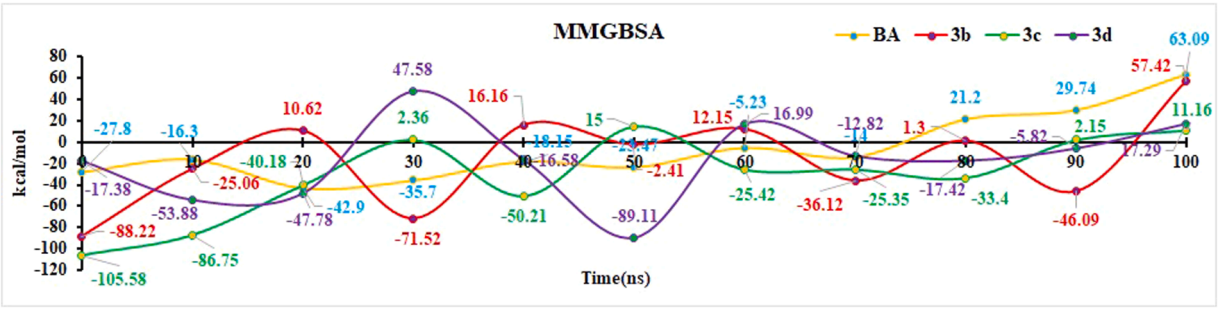

Fig. 13. MM-GBSA binding energy plot over run-time for all the complexes.

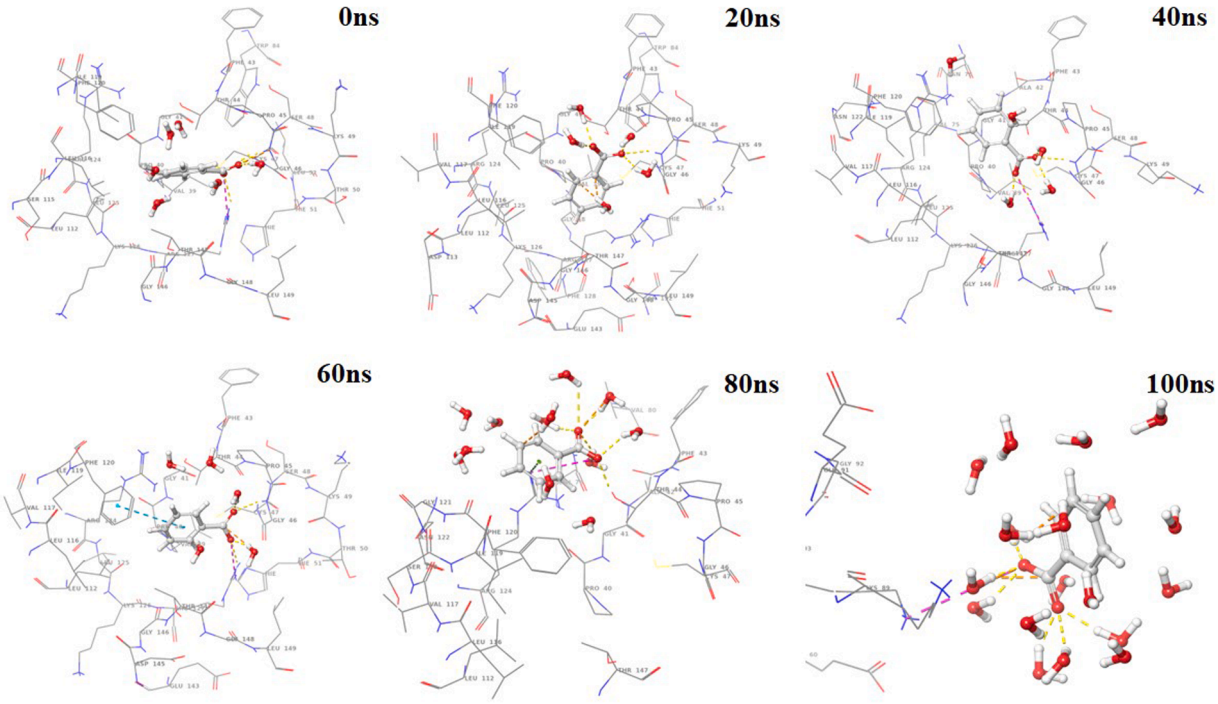

Fig. 14. Trajectory images of **BA**-PrxV during the 100 ns MDS.

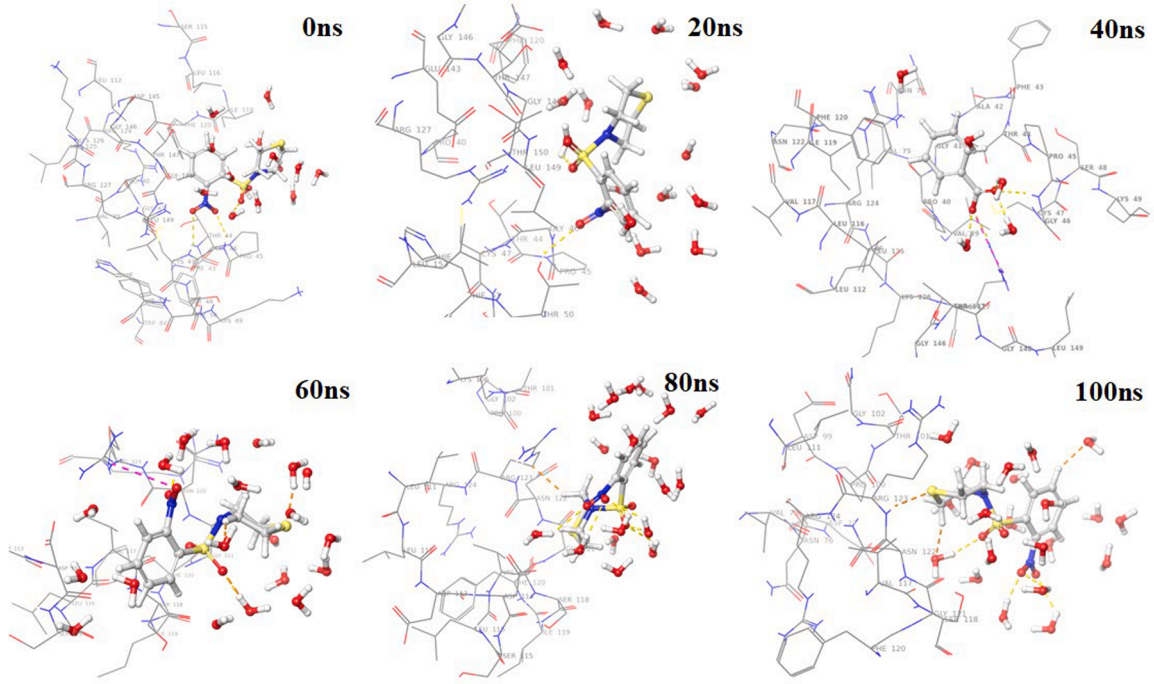

Fig. 15. Trajectory images of **3b** complex during 100 ns MDS.

regions in an MEP plot. MEPs represent the distributions of charge across the complete energy surface of the molecules. The molecule is more likely to be attacked by electrophiles in regions with high negative MEP (red or yellow), whereas nucleophiles are more likely to attack regions with high positive MEP (blue). It helps in used to identify potential sites for hydrogen bond interactions. MEPs are useful in determining behaviour of enzyme-substrate complex. Fig. 7 depicts the MEP of the optimized ligands.

3.6. Frontier molecular orbitals (FMOs)

Understanding of the Lowest Unoccupied Molecular Orbital (LUMO) and Highest Occupied Molecular Orbital (HOMO) are given by FMOs. Calculations of HOMO and LUMO were done using the molecular structure (optimized) of the compounds.

The presence of electron-withdrawing substituents (Halogens like F, Cl and NO_2) resulted in charge transfer towards the aromatic ring from HOMO (donor fragment) to LUMO (acceptor fragment) in all the

optimized structures. In case of molecules **3b** and **3d**, HOMO is found at one end of molecule and LUMO is found at other end, showing charge transfer through the molecules from one end to the other. Whereas, molecule **3c** showed localized HOMO-LUMO (both present in same region). Optimised molecules **3b, 3c,** and **3d** exhibited the highest biological activity as indicated by the lower energy gaps of 2.17, 4.23, and 1.21 eV (Fig. 8) [47].

3.7. Molecular docking studies

Peroxiredoxins (Prxs) are a class of Oxidoreductase enzymes. With a remarkably high catalytic efficiency, they engage in redox signalling and antioxidant defence, which makes them essential for cellular peroxide reduction. Some Prxs in eukaryotes are involved in the regulation of hydrogen peroxide signaling pathways in addition to their antioxidant action. Peroxiredoxins (Prxs) are vital peroxidases that use a conserved cysteine (Cys) residue to reduce peroxide substrates involved in redox signalling and antioxidant defence [48–50].

When compared with docking results of designed compounds **3b, 3c** and **3d** with PDBs for PrxV receptor, 1H4O (1.95 Å) and 1HD2 (1.50 Å) with the same cocrystal ligand benzoic acid (BA), we found that a similar kind of interactions between the ligands and the PrxV receptors. Docking results with PDB: 1H4O were comparatively better in terms of docking score as well as binding interactions with active site residues than with PDB: 1HD2. Thereby, we preferred to proceed with PDB 1H4O for our current study.

Re-docking benzoic acid (co-crystallized ligand) to its native position confirmed the docking protocol with the RMSD value of 0.0633 Å (Fig. 9). Further, by keeping all parameters the same, docking was done on all the synthesized compounds into the binding pockets of the targeted protein.

Co-crystallized ligand (BA) along with other antioxidant standard drugs like ascorbic acid, and quercetin, highly active compounds were analysed by the molecular docking technique to understand their binding affinities. Fig. 10 depicts the docking postures, and Table 3 outlines the docking score and interaction types with the PrxV receptor (PDB ID: 1H4O).

In comparison with the co-crystal ligand benzoic acid (BA), the docking score of all the active compounds is low, around −2 kcal/mol. Compound **3b** has a docking score of −2.012 kcal/mol, but it has produced similar binding interactions as the co-crystal ligand (BA) with the active site residues GLY 46, CYS 47, and ARG 127 of PrxV (PDB 1H4O). Furthermore, docking scores of the additional reference compounds, ascorbic acid and quercetin, were higher when compared with the most active compound **3b** Therefore, despite having low binding scores in comparison with co-crystal ligand benzoic acid (BA) and one of the reference compounds, ascorbic acid, the binding interaction given by compound **3b** is similar to that of these two compounds (BA and ascorbic acid).

3.8. Molecular dynamics simulations (MDS)

Simulations studies of the bound molecule (**3b**) with PDB 1H4O for 100 ns were performed to examine complex stability. PrxV receptor's backbone RMSD value at 2.95 ns, increased to 1.582 Å, and then by 43.75 ns, the value reduced to 1.055 Å. The **3b** complex, in the RMSD curve, exhibited a close match with BA (co-crystallized ligand) (Fig. 11A), indicating alignment and stability with the reference ligand. Mean RMSD value for receptor atoms was 2.541 Å and 1.880 Å for the PrxV receptor. Significant differences in the PrxV receptor's protein chain were found by root mean square fluctuation (RMSF) analysis (Fig. 11B), especially in the N- and C-terminal regions when compared to the other regions. These fluctuations indicate the conformational changes of the receptor on binding to BA, the reference ligand.

Compound BA, which demonstrated considerable docking scores, underwent 100 ns MD simulations to analyze the stability of the complex. Hydrogen-bonding and hydrophobic interactions were displayed by stable regions during simulation. BA demonstrated a stable radius of gyration (Rg) with an average value of 2.11 Å (Fig. 11C) and presented a high SASA during MDS.

Interactions with stability were seen at residues ARG 124, ALA 42, ASN 76, PHE 43, VAL 80, PHE 120, and ARG 127 in the simulation study of compound **3b** ALA 42, ARG 124, ASN 76, and ARG 127 formed hydrogen bonds. Also, hydrophobic interactions were exhibited by PHE 120. Hydrogen bonding interactions with the highest frequencies were exhibited by compound **3b** During the study, H-bond networks were observed for 27 % at ARG 127, and hydrophobic interactions for 7 % of the time with PHE 120. For stabilizing the PrxV-**3b** complex, no water-mediated H-bond networks contributed during simulation (Fig. 11D) [51].

The selection of a target for docking studies plays a crucial role in supporting the biological results obtained. Our target peroxiredoxins (Prxs) have remarkably high catalytic efficiency in redox signaling and antioxidant defence *via* a conserved cysteine (Cys) residue. The required interactions in the active site of PrxV by co-crystal ligand BA which are essential for anti-oxidant activity, were also observed in case of compound **3b** with active site residue Cys 47 in molecular docking and MD simulation, thereby supporting the potent anti-oxidant activity shown in biological studies.

The secondary structural and torsional profiles of the **PrxV-3b** complex are presented in Fig. 12. Ligand properties of the simulated compounds **3b, 3c** and **3d** are outlined in Table 4. **Figures S20–S27** present the interaction graphs and secondary structural properties of the compounds **3c, 3d** and BA during MDS.

3.9. Estimation of binding-free energy

To compute binding free energies, MM-GBSA studies were performed on complexes from docking and dynamic simulations. Stronger protein-ligand interactions are indicated by lower binding energy values, explaining improved binding affinity. Specifically, the BA (co-crystallized ligand) displayed maximum binding energy. The total binding energies (ΔG) after docking was −22.94 kcal/mol for **BA**, for **3b** it was −29.12 kcal/mol, −30.33 kcal/mol for compound **3c**, and for compound **3d** it was −39.19 kcal/mol.

Binding free energies for 3b, 3c, 3d, and BA pre-MD simulations and post-MD simulations are outlined in Table 5. Protein residues contributing to the lowest binding energy include ASN 76, PHE 120, ALA 42, ARG 124, VAL 80, PHE 43, and ARG 127.

In case of post MD MMGBSA analysis, co-crystal ligand BA showed the highest binding energy (−6.32 kcal/mol) in all of them because of the maximum instability of the ligand in the active site. The **3b** complex displayed an average ΔG binding energy of −15.61 kcal/mol, while **3d** exhibited −16.26 kcal/mol. Minimum binding energy of −30.56 kcal/mol was shown by the **3c** complex. Fig. 13 depicts the binding energy plot for all the complexes.

Post-simulation MMGBSA analysis was performed on BA-1H4O complex to check the stability of the complex in terms of binding free energy throughout the course of simulation. In trajectory analysis (Fig. 14), it was observed that the co-crystal ligand came out of the binding pocket, because of missing binding interactions with active site key residues such as GLY 46, CYS 47, and ARG 127 over period of time somewhere around 76.35 ns to the end of the MD simulation, which led the MMGBSA value to shift drastically.

Post-simulation binding free energy was calculated as the average of all the binding free energies of protein-ligand complex at particular intervals throughout simulation. When the average was taken, there was a decrease in binding free energy of post-MD **3d**-1H4O complex in comparison with the pre-MD **3d**-1H4O complex. The MMGBSA value was decreased from −39.19 kcal/mol to −16.26 kcal/mol, making it less stable.

The fluctuations were seen less in case of compound **3b** over co-

crystal BA while analyzing MD simulation trajectory snapshots (Fig. 15) but when compared with the co-crystal ligand benzoic acid i.e., BA-PrxV complex, it was found to be more stable. Docking followed by dynamic results disclosed that effective binding interactions with receptor (PrxV) was exhibited by **3b** compound. By presenting good stability during the simulations, the **3b** compound can be the lead for binding at the active site of PrxV.

4. Conclusion

A new series of novel thiomorpholine-bearing sulfonamides were synthesized in good to excellent yields (87–95 %). To the best of our knowledge, this study gives the synthesis of thiomorpholine-containing sulfonamides as potentially effective antioxidant drug candidates. In both H_2O_2 and DPPH radical scavenging methods, compounds **3b, 3c** and **3d** shown significant antioxidant activity compared with the standard drug, ascorbic acid. These compounds with the highest percentage of inhibition presented lower IC_{50} values, as it indicates that minimum amounts were required to achieve 50 % inhibition, and these values were comparable to those of a standard drug, ascorbic acid. *In-silico* ADME results validated the drug-like properties of all the compounds as they obeyed Lipinski's rule. Computational analysis revealed the stability followed by strong binding affinity of the **PrxV-3b** complex. *In-vitro* results were validated by the binding studies of **3b** complex at the active site of PrxV receptor. Future research should focus on optimizing the structural features of these sulfonamide analogs to enhance their binding affinities, biological activity, and drug-likeness, including solubility, stability, and bioavailability. Experimental validation through comprehensive *in-vitro* and *in-vivo* studies are essential to evaluate their antioxidant potential, pharmacokinetics, toxicity, and overall safety.

CRediT authorship contribution statement

C.R. Santhosh: Conceptualization, Data curation, Formal analysis, Resources, Writing – original draft, Writing – review & editing. **Sampath Chinnam:** Conceptualization, Supervision, Methodology, Resources, Formal analysis, Writing – original draft, Writing – review & editing. **Hrushikesh S. Chaudhari:** Conceptualization, Data curation, Formal analysis, Resources, Writing – original draft, Writing – review & editing. **Kondapalli Venkata Gowri Chandra Sekhar:** Conceptualization, Supervision, Methodology, Resources, Formal analysis, Writing – original draft, Writing – review & editing. **Gbolahan O. Oduselu:** Writing – review & editing. **Vishal Ahuja:** Conceptualization, Supervision, Methodology, Resources, Formal analysis, Writing – original draft, Writing – review & editing. **Kumarappan Chidambaram:** Writing – review & editing. **Nagaraju Kerru:** Conceptualization, Supervision, Methodology, Resources, Formal analysis, Writing – original draft, Writing – review & editing. **G.M. Madhu:** Writing – review & editing.

Declaration of competing interest

The authors declare that they have no known competing financial interests or personal relationships that could have appeared to influence the work reported in this paper.

Acknowledgments

The authors are grateful to the M. S. Ramaiah Institute of Technology, Bengaluru 560054, Karnataka, India under the SEED money project: MSRIT/Admin/1575/23–24. The authors extend their appreciation to the Deanship of Scientific Research at King Khalid University, Saudi Arabia for supporting this work through a Large Group Research Project under grant number RGP.2/189/46. The author C. R. Santhosh is grateful to M.S. Ramaiah Institute of Technology, Bengaluru 560054, Karnataka, India, for the fellowship support through Ramaiah Doctoral Fellowship.

Supplementary materials

Supplementary material associated with this article can be found, in the online version, at doi:10.1016/j.molstruc.2025.143201.

Data availability

No data was used for the research described in the article.

References

[1] N. Chandimali, S.G. Bak, E.H. Park, H.J. Lim, Y.S. Won, E.K. Kim, S.I. Park, S.J. Lee, Free radicals and their impact on health and antioxidant defenses: a review, Cell Death Discov. (2025), https://doi.org/10.1038/s41420-024-02278-8.
[2] K. Nakai, D. Tsuruta, What are reactive oxygen species, free radicals, and oxidative stress in skin diseases? Int. J. Mol. Sci. (2021) https://doi.org/10.3390/ijms221910799.
[3] D. Bešlo, N. Golubić, V. Rastija, D. Agić, M. Karnaš, D. Šubarić, B. Lučić, Antioxidant activity, metabolism, and bioavailability of polyphenols in the diet of animals, Antioxidants (2023), https://doi.org/10.3390/antiox12061141.
[4] B. Halliwell, Understanding mechanisms of antioxidant action in health and disease, Nat. Rev. Mol. Cell Biol. (2024), https://doi.org/10.1038/s41580-023-00645-4.
[5] B. Poljsak, V. Kovač, I. Milisav, Antioxidants, food processing and health, Antioxidants (2021), https://doi.org/10.3390/antiox10030433.
[6] M. Parcheta, R. Świsłocka, S. Orzechowska, M. Akimowicz, R. Choińska, W. Lewandowski, Recent developments in effective antioxidants: the structure and antioxidant properties, Materials (2021), https://doi.org/10.3390/ma14081984.
[7] A.M. Pisoschi, A. Pop, F. Iordache, L. Stanca, G. Predoi, A.I. Serban, Oxidative stress mitigation by antioxidants-an overview on their chemistry and influences on health status, Eur. J. Med. Chem. (2021), https://doi.org/10.1016/j.ejmech.2020.112891.
[8] M. Kurek, N. Benaida-Debbache, I. Elez Garofulić, K. Galić, S. Avallone, A. Voilley, Y. Waché, Antioxidants and bioactive compounds in food: critical review of issues and prospects, Antioxidants (2022), https://doi.org/10.3390/antiox11040742.
[9] S. Asirvatham, E. Thakor, H. Jain, T. Morpholine, Privileged scaffold possessing diverse bioactivity profile, J. Chem. Rev. (2021), https://doi.org/10.22034/JCR.2021.295839.1123.
[10] J. Wei, L. Chen, K. Zhu, Y.X. Cheng, D. Huang, Design, synthesis, and fungicidal activity evaluation of 2-methyl-5-phenylthiazole-4-carboxamides bearing morpholine, thiomorpholine, or thiomorpholine 1, 1-dioxide moiety, Chem. Heterocycl. Compd. (2024), https://doi.org/10.1007/s10593-024-03372-6.
[11] N. Chirra, V. Shanigarapu, N.P. Abburi, E.O. Sinegubova, R.K. Pedapati, Y. L. Esaulkova, V.V. Zarubaev, S. Kantevari, Synthesis and antiviral activity of novel imidazo [2, 1-b] thiazoles coupled with morpholine and thiomorpholines, J. Heterocycl. Chem. (2024), https://doi.org/10.1002/jhet.4778.
[12] P. Theodosis-Nobelos, G. Papagiouvannis, E.A. Rekka, Ferulic, sinapic, 3, 4-dimethoxycinnamic acid and indomethacin derivatives with antioxidant, anti-inflammatory and hypolipidemic functionality, Antioxidants (2023), https://doi.org/10.3390/antiox12071436.
[13] W. Zafar, S.H. Sumrra, A.U. Hassan, Z.H. Chohan, A review on sulfonamides: their chemistry and pharmacological potentials for designing therapeutic drugs in medical science, J. Coord. Chem. (2023), https://doi.org/10.1080/00958972.2023.2208260.
[14] Y. Cao, S. Abdolmohammadi, R. Ahmadi, A. Issakhov, A.G. Ebadi, E. Vessally, Direct synthesis of sulfenamides, sulfinamides, and sulfonamides from thiols and amines, RSC Adv. (2021), https://doi.org/10.1039/D1RA04368D.
[15] S.B. Christensen, Drugs that changed society: History and current status of the early antibiotics: Salvarsan, sulfonamides, and β-lactams, Molecules (2021), https://doi.org/10.3390/molecules26196057.
[16] Y. Wan, G. Fang, H. Chen, X. Deng, Z. Tang, Sulfonamide derivatives as potential anti-cancer agents and their SARs elucidation, Eur. J. Med. Chem. (2021), https://doi.org/10.1016/j.ejmech.2021.113837.
[17] M.U. Rahman, H.M. Javed, S. Hassan, T. Munir, R. Asghar, Exploring sulfonamides derivatives schiff base and metal complexes as antimicrobial agents: a comprehensive review, Inorg. Chem. Commun. (2024), https://doi.org/10.1016/j.inoche.2024.113396.
[18] K.A. Elsayad, G.F. Elmasry, S.T. Mahmoud, F.M. Awadallah, Sulfonamides as anticancer agents: a brief review on sulfonamide derivatives as inhibitors of various proteins overexpressed in cancer, Bioorg. Chem. (2024), https://doi.org/10.1016/j.bioorg.2024.107409.
[19] P. Chen, J. Yang, Y. Zhou, X. Li, Y. Zou, Z. Zheng, M. Guo, Z. Chen, W.J. Cho, N. Chattipakorn, W. Wu, Design, synthesis, and bioactivity evaluation of novel amide/sulfonamide derivatives as potential anti-inflammatory agents against acute lung injury and ulcerative colitis, Eur. J. Med. Chem. (2023), https://doi.org/10.1016/j.ejmech.2023.115706.
[20] C.A. Salubi, Research progress in HIV and mycobacterium tuberculosis inhibitors containing sulfonamide moiety, J. Chem. (2023), https://doi.org/10.1155/2023/3601764.
[21] Sreerama R., N V.R., Narsimha S. (2020) One-pot synthesis of sulfonyl-1 H-1, 2, 3-triazolyl-thiomorpholine 1, 1-dioxide derivatives and evaluation of their biological activity. Phosphorus, sulfur, silicon relat. Elem. https://doi.org/10.1080/10426507.2020.1854257.

[22] J.I. Levin, J.M. Chen, L.M. Laakso, M. Du, J. Schmid, W. Xu, T. Cummons, J. Xu, G. Jin, D. Barone, J.S. Skotnicki, Acetylenic TACE inhibitors. Part 3: thiomorpholine sulfonamide hydroxamates, Bioorg. Med. Chem. Lett. (2006), https://doi.org/10.1016/j.bmcl.2005.12.020.
[23] A. Ovung, J. Bhattacharyya, Sulfonamide drugs: structure, antibacterial property, toxicity, and biophysical interactions, Biophys. Rev. (2021), https://doi.org/10.1007/s12551-021-00795-9.
[24] J. Soni, N. Sahiba, A. Sethiya, S. Agarwal, Polyethylene glycol: a promising approach for sustainable organic synthesis, J. Mol. Liq. (2020), https://doi.org/10.1016/j.molliq.2020.113766.
[25] M.M. Hoffmann, Polyethylene glycol as a green chemical solvent, Curr. Opin. Colloid Interface Sci. (2022), https://doi.org/10.1016/j.cocis.2021.101537.
[26] W. Li, J. Wu, J. Zhang, J. Wang, D. Xiang, S. Luo, J. Li, X. Liu, Puerarin-loaded PEG-PE micelles with enhanced anti-apoptotic effect and better pharmacokinetic profile, Drug Deliv. (2018), https://doi.org/10.1080/10717544.2018.1455763.
[27] N.M. Panchani, K.M. Kapadiya, H.S. Joshi, A green approach for the catalyst-free synthesis of imidazole-bearing pyrazole moiety using PEG-400 as an efficient recyclable medium as potential anti-tubercular and anti-microbial agents, J. Heterocycl. Chem. (2022), https://doi.org/10.1002/jhet.4543.
[28] A.D. Kale, R.H. Pawara, H.M. Patel, D.S. Dalal, A facile and efficient one-pot procedure for the synthesis of 2-amino-4, 8-dihydropyrano [3, 2-b] pyran-3-carbonitriles in PEG-400 and glycerol, Res. Chem. Intermed. (2024), https://doi.org/10.1007/s11164-023-05188-z.
[29] F. Stanzione, I. Giangreco, J.C. Cole, Use of molecular docking computational tools in drug discovery, Prog. Med. Chem. (2021), https://doi.org/10.1016/bs.pmch.2021.01.004.
[30] H. Komura, R. Watanabe, K. Mizuguchi, The trends and future prospective of in silico models from the viewpoint of ADME evaluation in drug discovery, Pharm. (2023), https://doi.org/10.3390/pharmaceutics15112619.
[31] U. Naithani, V. Guleria, Integrative computational approaches for discovery and evaluation of lead compound for drug design, Front. Drug Discov. (2024), https://doi.org/10.3389/fddsv.2024.1362456.
[32] N.S. Blunt, J. Camps, O. Crawford, R. Izsák, S. Leontica, A. Mirani, A.E. Moylett, S. A. Scivier, C. Sunderhauf, P. Schopf, J.M. Taylor, Perspective on the current state-of-the-art of quantum computing for drug discovery applications, J. Chem. Theory Comput. (2022), https://doi.org/10.1021/acs.jctc.2c00574.
[33] A.V. Sadybekov, V. Katritch, Computational approaches streamlining drug discovery, Nature (2023), https://doi.org/10.1038/s41586-023-05905-z.
[34] M. Burits, F. Bucar, Antioxidant activity of Nigella sativa essential oil, Phytother. Res. (2000), https://doi.org/10.1002/1099-1573(200008)14:5&3C323::AID-PTR621&3E3.0.CO;2-Q.
[35] R.J. Ruch, S.J. Cheng, J.E. Klaunig, Prevention of cytotoxicity and inhibition of intercellular communication by antioxidant catechins isolated from Chinese green tea, Carcinogenesis (1989), https://doi.org/10.1093/carcin/10.6.1003.
[36] A. Daina, O. Michielin, V. Zoete, SwissADME: a free web tool to evaluate pharmacokinetics, drug-likeness and medicinal chemistry friendliness of small molecules, Sci. Rep. (2017), https://doi.org/10.1038/srep42717.
[37] D.E. Pires, T.L. Blundell, D.B. Ascher, pkCSM: predicting small-molecule pharmacokinetic and toxicity properties using graph-based signatures, J. Med. Chem. (2015), https://doi.org/10.1021/acs.jmedchem.5b00104.
[38] Frisch M.J. Gaussian 09, Revision D. 01/Gaussian.
[39] Dennington R., Keith T., Millam J. GaussView, version 5.
[40] H.M. Berman, J. Westbrook, Z. Feng, G. Gilliland, T.N. Bhat, H. Weissig, I. N. Shindyalov, P.E. Bourne, The protein data bank, Nucleic Acids Res. (2000), https://doi.org/10.1093/nar/28.1.235.
[41] A. Hall, D. Parsonage, L.B. Poole, P.A. Karplus, Structural evidence that peroxiredoxin catalytic power is based on transition-state stabilization, J. Mol. Biol. (2010), https://doi.org/10.1016/j.jmb.2010.07.022.
[42] Maestro, Schrödinger Release 2024-4: Maestro, Schrödinger, LLC, New York, NY, 2024.
[43] R.A. Friesner, R.B. Murphy, M.P. Repasky, L.L. Frye, J.R. Greenwood, T.A. Halgren, P.C. Sanschagrin, D.T. Mainz, Extra precision glide: docking and scoring incorporating a model of hydrophobic enclosure for protein− ligand complexes, J. Med. Chem. (2006), https://doi.org/10.1021/jm051256o.
[44] Desmond, Schrödinger Release 2024-4: Desmond Molecular Dynamics System, D. E. Shaw Research, New York, NY, 2024. Maestro-Desmond Interoperability Tools, Schrödinger, New York, NY, 2024.
[45] C. Lu, C. Wu, D. Ghoreishi, W. Chen, L. Wang, W. Damm, G.A. Ross, M.K. Dahlgren, E. Russell, C.D. Von Bargen, R. Abel, OPLS4: improving force field accuracy on challenging regimes of chemical space, J. Chem. Theory Comput. (2021), https://doi.org/10.1021/acs.jctc.1c00302.
[46] Prime, Schrödinger Release 2024-4: Prime, Schrödinger, LLC, New York, NY, 2024.
[47] S. Muhammad, A. Faiz, S. Bibi, S.U. Rehman, M.Y. Alshahrani, Investigation of dual inhibition of antibacterial and antiarthritic drug candidates using combined approach including molecular dynamics, docking and quantum chemical methods, Comput. Biol. Chem. (2024), https://doi.org/10.1016/j.compbiolchem.2024.108218.
[48] Z.A. Wood, E. Schröder, J.R. Harris, L.B. Poole, Structure, mechanism and regulation of peroxiredoxins, Trends. Biochem. Sci. (2003), https://doi.org/10.1016/S0968-0004(02)00003-8.
[49] N.M. Ahmed, A.H. Lotfallah, M.S. Gaballah, S.M. Awad, M.K. Soltan, Novel 2-thiouracil-5-sulfonamide derivatives: design, synthesis, molecular docking, and biological evaluation as antioxidants with 15-LOX inhibition, Molecules (2023), https://doi.org/10.3390/molecules28041925.
[50] S. Jorepalli, S. Adikay, R.R. Chinthaparthi, C.S. Gangireddy, J.R. Koduru, R. R. Karri, Synthesis, molecular docking studies and biological evaluation of N-(4-oxo-2-(trifluoromethyl)-4 H-chromen-7-yl) benzamides as potential antioxidant, and anticancer agents, Sci. Rep. (2024), https://doi.org/10.1038/s41598-024-59166-5.
[51] S. Bathula, M. Sankaranarayanan, B. Malgija, I. Kaliappan, R.R. Bhandare, A. B. Shaik, 2-Amino thiazole derivatives as prospective aurora kinase inhibitors against breast cancer: QSAR, ADMET prediction, molecular docking, and molecular dynamic simulation studies, ACS Omega (2023), https://doi.org/10.1021/acsomega.3c07003.